Impact of Transceiver Alignment on a Software-defined Underwater Visible Light Communication System

Sana Rehman
School EECMS
Curtin University
Bentley,WA, Australia
sana.rehman@student.curtin.edu.au

Yue Rong
School EECMS
Curtin University
Bentley,WA, Australia
y.rong@curtin.edu.au

Peng Chen
School EECMS
Curtin University
Bentley,WA, Australia
peng.chen@curtin.edu.au

2024 IEEE 29th Asia Pacific Conference on Communications (APCC) | 979-8-3315-1781-6/24/$31.00 ©2024 IEEE | DOI: 10.1109/APCC62576.2024.10767906

***Abstract*—Underwater visible light communication (UVLC) is believed to revolutionize the future of optical communication, where visible light of wavelength 400-500 nm range is used to transmit data underwater. In this paper we aim to find how the position of the receiver affects the accuracy of the received optical signal. The message signal is modulated using pulse position modulation (PPM) because of its high noise resistance through water. The position of the receiver is changed accordingly and the bits in error are recorded to discuss the relationship between angle of the receiver, bit-error-rate and received signal power.**

***Index Terms*—Underwater visible light communication, Software-defined radio, Pulse position modulation.**

I. Introduction

Underwater communication attracts many researchers because of the growing underwater human activities [1]. To date underwater acoustic communication has remained the dominant mode due to long link distance up to tens of kilometres, but it has low data rate, requires power hungry transceivers and has poor bandwidth efficiency [2]. On the other hand radio frequency (RF) communication has good data rate but suffers from attenuation because water behaves like a conductor for RF wave. Moreover, it requires huge antennas along with high power consumption and expensive installation [3]. Using optical or visible light as an alternative also has a drawback like short link range [4], but it has high bandwidth efficiency, does not require expensive transceivers and supports high data rate. Because of an added advantage of being safe for marine life [5], research in underwater visible light communication (UVLC) has been increased over the past decades to mitigate the shortcomings and get the benefit from this mode of communication. Figure 1 shows the rate-range of different underwater communication approaches [6].

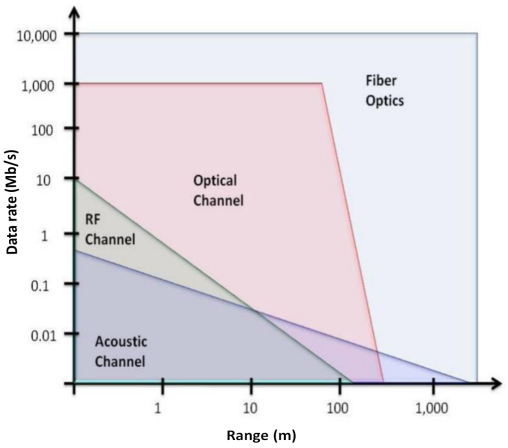

Fig. 1. Comparative performance of different underwater communication approaches [6].

II. UVLC Channel

Whenever light travels in an aquatic medium it suffers from absorption and scattering. Absorption is an irreversible process where photons lose energy thermally, whereas in scattering they change their direction upon interaction with water molecules and suspended particles [7]. Both are wavelength dependent. These two parameters contribute to beam divergence angle which is defined as an angular measurement and is expressed as a divergence angle in radians [8]. The beam is diverged because of scattering as shown in Figure 2.

If transmitter and receiver are not aligned and the light wavelength is not chosen wisely the inherent parameters

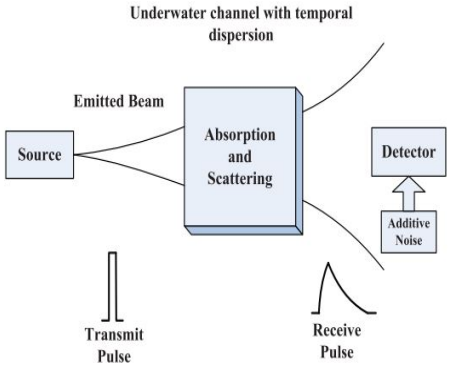

Fig. 2. System model and link geometry of the UVLC link [6].

of water like absorption and scattering can cause loss of information. Hence, in this paper our focus is to find the impact of angular displacement of the receiver on the communication link.

III. System Model

There are several models proposed for UVLC system that lead to finding channel impulse response determining not only the quality of channel but also the signal received. Beer's law is the simplest one, which considers the linear motion of photons. Optical power (I) after a distance (z), based on the transmitted power (I_o) is given by

$$I = I_o e^{-cz} \tag{1}$$

where c is the extinction coefficient (sum of absorption and scattering coefficients) and z is the link range. The stochastic model follows the analytical approach to compute the probabilistic value of scattering (also known as scattering function). Henyey–Greenstein (HG) function is used in this model to deduce the scattering phase function which is critical in finding the pathloss and signal quality at the receiving end. The detailed discussion is given in [9]- [11]. The HG equation is given by [12], [13]

$$P_{HG}(\theta) = \frac{1-g^2}{4\pi(1+g^2-2gcos(\theta))^{3/2}} \tag{2}$$

where P_{HG} is the probability density function of the scattering phase function and g is particle asymmetry factor which depends on the medium characteristics and is equal to the average of $cos(\theta)$. The scattering angle θ can be found by [13]

$$\theta = cos^{-1}(\frac{1}{2g}[1+g^2-(\frac{1-g^2}{1+g-2g\xi})^2]) \tag{3}$$

where ξ is a random variable between 0 and 1.

From the scattering angle the power at the receiver P_r can be deduced as [14]

$$P_r = \frac{P_t e^{-cz} D^2 cos(\phi)}{4z^2 tan^2(\theta)} \tag{4}$$

where P_t is the transmitted power, θ is the scattering angle, D is the diameter of the receiver, ϕ is the inclination angle (angle between the receiver's normal w.r.t. light beam) [14]. Quality of the signal is determined by its SNR S at the receiver which is given by:

$$S = \frac{P_r^2}{P_{noise}^2}; \tag{5}$$

where P_{noise} denotes the noise power. The SNR S can be used to find the bit-error-rate (BER). Different modulation schemes have different BER formula. The BER for the PPM is given by [15]

$$\eta_{BER} = \frac{1}{2} erfc\Big[\frac{1}{2\sqrt{2}}\sqrt{\frac{SLlog_2 L}{2}}\Big] \tag{6}$$

where L is the PPM level (number of slots needed to encode the message bits) and $erfc$ is the complimentary error function which is given by [16] [17].

$$erfc = (2\pi)^{-1/2} \int_x^\infty e^{-t^2}\, dt. \tag{7}$$

IV. UVLC System Hardware

The hardware setup for the system can be seen in Figures 3 and 4. Modulated 4-PPM and 8-PPM signals are created in MATLAB which is configured with USRP NI-2920. This signal is transmitted via visible light of wavelength around 450 nm through LIFI transceivers separated by a water tank of length, width and height of 36 cm, 26 cm and 22.5 cm respectively.

A. Angular Position of Receiver

The angular position for line-of-sight (LOS) communication and non-line-of-sight (NLOS) communication is shown in Figure 5 and Figure 6 respectively. The receiver position is changed w.r.t. different angles marked whereas the transmitter is fixed at 0^o and 20^o for LOS and NLOS communication respectively. The transmitter and receiver are separated by a water tank.

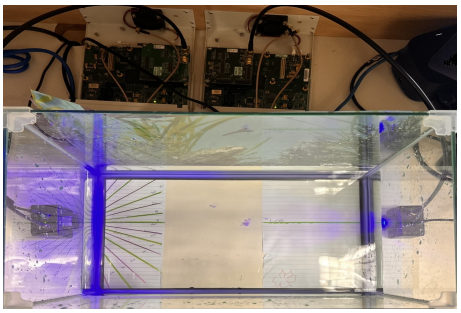

Fig. 3. Hardware setup for UVLC.

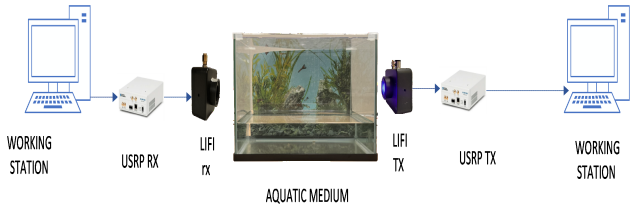

Fig. 4. Block diagram for UVLC.

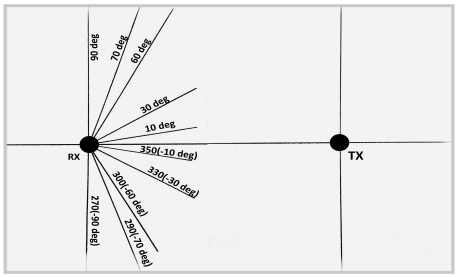

Fig. 5. LOS angular position of the receiver w.r.t. transmitter.

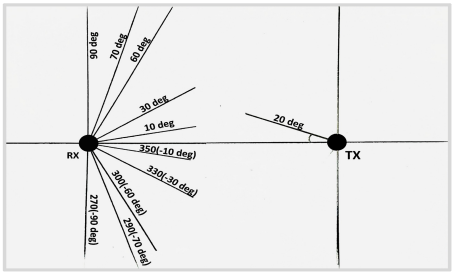

Fig. 6. NLOS angular position of the receiver w.r.t. transmitter.

V. System Design

A. Transmitting Station Design

The transmitting station flow chart can be seen in Figure 7.

1) Transmitter: The transmitter consists of a host computer with MATLAB installed to create the message signal. While designing the transmitter the problem of

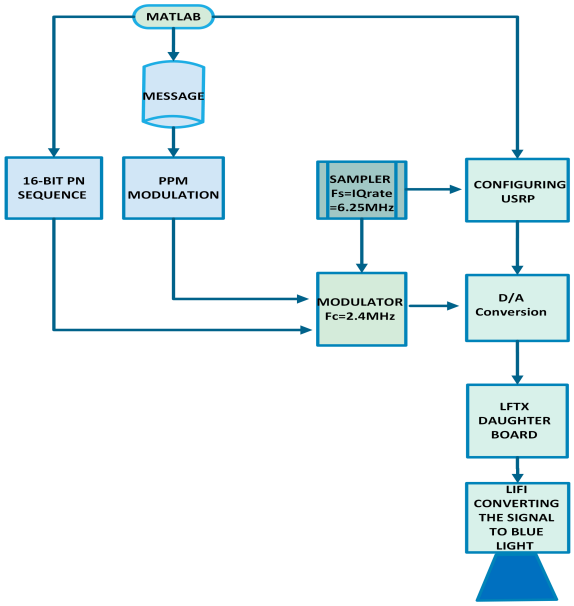

Fig. 7. Flow chart for transmitting station.

underrun was encountered. This problem occurs when the writing speed of the host is slower than the reading speed of the NI-USRP 2920. Not only it depends on the processing speed of the working station but also the interpolation factor (IF) of the radio device. The IF is chosen critically to not only accommodate the frequency of the tone signal but address the reading speed of the USRP.

2) Frame Structure: The transmission frame consists of the preamble and the payload. A 16-bit modulated pseudonoise (PN) sequence is used as a preamble whereas the payload is the PPM signal. Both the payload and the preamble are modulated with 2.4 MHz tone signal. The frame structure is shown in Figure 8 below.

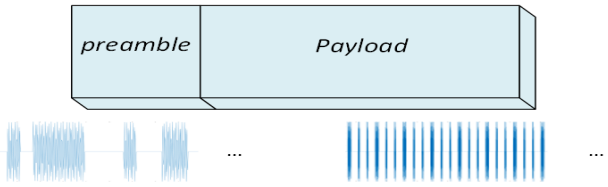

Fig. 8. Frame structure for UVLC system.

3) Modulation Scheme: PPM is a digital modulation technique in which a message signal is encoded in 2^M possible slots where M is the number of message bits. PPM is used due to low transmit power and better noise performance [18].

4) Low Frequency Transmit (LFTX) Daughter Board: The modulated signal after passing through the digi-

tal to analogue convertor is filtered and upconverted at the daughter board for passband transmission [19]. NI USRP-2920 comes with wide bandwidth transceiver (WBX) daughter board which works in the frequency range of 50 MHz to 2.2 GHz. Since the desired operating frequency for this particular UVLC system is under 50 MHz the low frequency daughter board is used. This daughter board unlike WBX does not have a local oscillator that could contribute to phase noise.

5) Optical Transceivers: LIFI R&D kit containing transmitter and receiver module from HYPERION Technologies was used. The module offers 20 MHz bandwidth and has a 170 degrees detector field of view. One Watt blue LED is used to transmit the PPM signal via water. The analogue signal from USRP is sent to an optical transmitter front-end, which adds DC bias, converts the electrical signal to blue light, and transmits the resulting signal through underwater optical channel [20]. The position of the transmitter was fixed whereas the receiver was moved consistently.

6) Carrier Frequency: There are two methods to transmit the baseband PPM signal. The first one is to modulate the signal with a carrier whose sampling frequency matches the IQ rate of the USRP and the second one is to initialize the carrier frequency of the software-defined radio (SDR) object and transmit the baseband PPM signal. The latter one is not the right choice, since the received signal is already demodulated with unknown offset which can be difficult to calculate. Choosing the carrier frequency of a modulating signal is challenging since the configuration of USRP and LIFI can be severely affected if the frequency is not chosen within their operating range. After carefully observing the response of the SDR and LIFI, 2.4 MHz is chosen as the optimum carrier frequency. This not only addresses the underrun issue where the writing speed of the PC and the reading speed of the USRP results in halting the transmission but also helps the optical transceivers to accurately deliver the signal to the receiving end. 2.4 MHz carrier frequency is good enough to choose the interpolation factor of 16 corresponding to the sampling frequency of 6.25 MHz.

B. Receiving Station Design

The receiver design is similar to transmitter as can be seen in Figure 9, with LIFI RX passing the received data into the A/D convertor of USRP via low frequency receive (LFRX) daughter board. The data is then passed to the MATLAB for all the signal processing. At the receiver end the choice of samples per frames G is important. G is chosen such that the USRP runs till all the information is fetched into the buffer. G at the receiver end and interpolation factor (IF) at transmitting end are inversely related, decreasing the IF means increasing the samples per frame parameter of the receiver USRP. During the design, two problems were encountered, the first one was the overflow and the second one was the offset frequency.

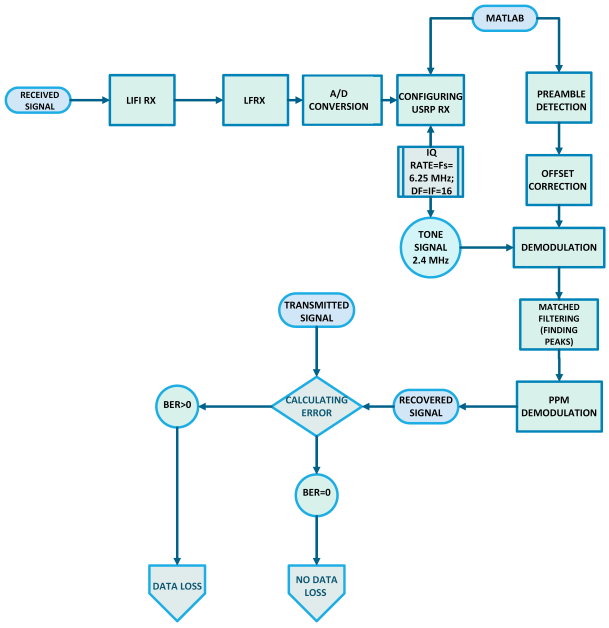

Fig. 9. Flow chart for receiving station.

1) Overflow: Overflow occurs when the reading speed of the host computer is less than the writing speed of the USRP buffer. Choosing the right working station along with G and the decimation factor is important. Overflow was detected after sorting the last two parameters because of the memory constraint of the receiving work station. It was observed that the processing speed of the receiving station should be greater than or equal to the transmitting station to avoid this issue.

2) Offset Frequency: The nominal master clock at each USRP is fixed at 100 MHz. However, a slight mismatch between the master clocks at the transmitter and receiver leads to carrier frequency offset. It is constant and can be easily estimated and removed. The frequency of received signal is 2.4046 MHz. The frequency spectrum can be seen in Figure 10.

3) Matched Filter: A matched filter is designed with the pulse width equal to the slot duration of PPM and relevant peaks are obtained using cross correlation. The peaks are translated to the respective bits. After retrieving received bits, the BER is calculated.

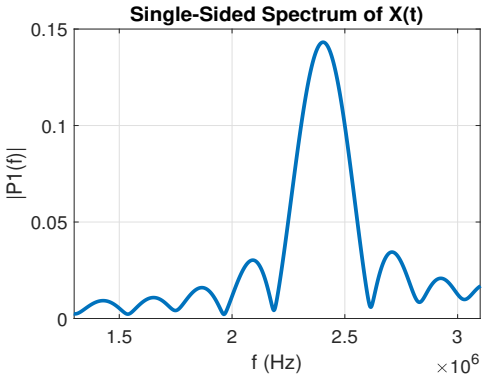

Fig. 10. Single-sided frequency spectrum for the received signal.

4) Computational Complexity: The receiver design can be implemented with a low computational complexity, as all operations shown in 9 can be computed efficiently. The signals received by the USRP are first cross correlated with a 16-bit PN preamble sequence to determine the starting point of the signal received. Once the preamble is detected, the next task is to find the frequency offset. A 2048-point FFT is performed on the sequence to determine the frequency offset. The corrected carrier frequency is used to demodulate the received signal. Once the signal is demodulated, it is filtered through a 20th order low pass filter with a Hann window (since it provides better stopband rejection). Finally, the message bits are extracted through convolution with a rectangular pulse with a duration equal to the transmitted bit duration. We can see that all the receiver operations have a low complexity.

VI. Results

Transmitting via LIFI was a challenge, after several trials 223.2 kHz PPM signal was sent at a carrier frequency of 2.4 MHz for optimum signal reception. Initially the experiment was carried out with air as a medium and later replaced with aquatic medium. Upon proper alignment, the receiver position was changed at various angles to find its effect on BER and received power of a signal for different levels of PPM.

As can be seen from Figure 11, the BER is zero from -30^o onwards till 40^o i.e. when the transmitter and receiver are following strict alignment but when the receiver is moving towards right or left beyond -30^o and 40^o, the BER begins to increase to an extent where it is maximum at perpendicular position to the transmitter. 8-PPM shows high BER for the same angular position than 4-PPM.

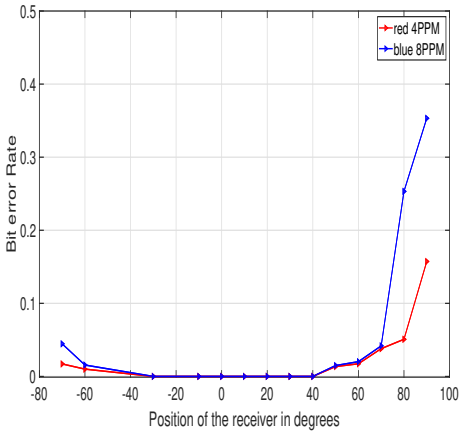

Fig. 11. Relationship between BER and the position of the receiver for LOS communication.

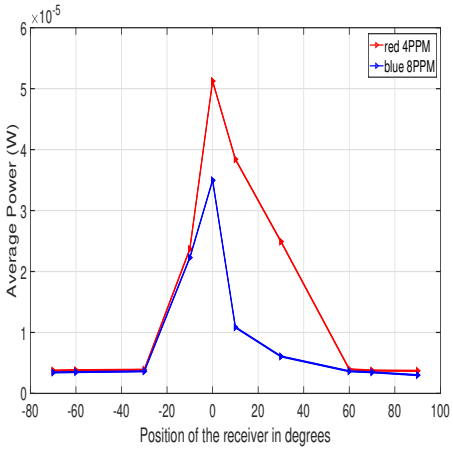

Fig. 12. Relationship between average received power and the position of the receiver for LOS communication.

Figure 12 shows that power of a signal is low when the receiver is not aligned and maximum at 0^o i.e. when the transmitter and receiver are perfectly aligned. Also, the graph suggests 4-PPM has more power than 8-PPM as the former transmits once every 4 slots, as compared to the latter which transmits once in every 8 slots.

Figures 13 and 14 show the BER and received power for NLOS communication respectively. The experiment for NLOS was carried out the same way as LOS. The transmitter was kept at 20^o w.r.t. LOS distance between transmitter and receiver whereas the receiver position was changed consistently. Figure 13 shows that BER begins to increase when the transmitter angle of incidence is out of receiver's field of view (FOV), but as soon as the beam is incident within the FOV of receiver the BER begins to decrease. In Figure 14, the received

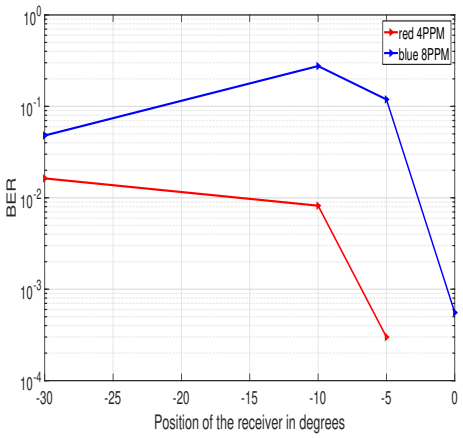

Fig. 13. Relationship between BER and the position of the receiver for NLOS communication.

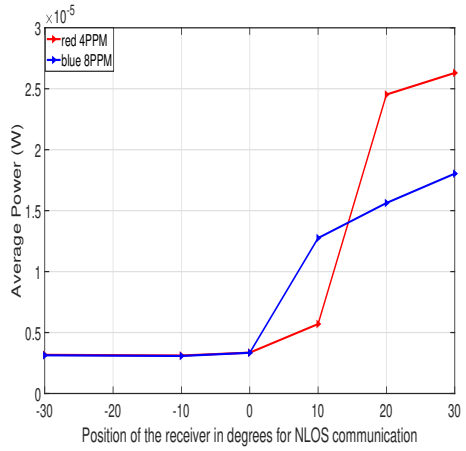

Fig. 14. Relationship between average received power and the position of the receiver for NLOS communication

power for NLOS communication is minimum when the incident beam is out of receiver's FOV but it increases as the transmitter and receiver are achieving alignment.

VII. Conclusion

UVLC is the future of underwater communication, where the receiver and transmitter positions are very critical to the accuracy of the data. PPM is a smart way to retain the accuracy of the message signal without compromising the noise efficiency of the UVLC system, but choosing the right level of PPM is necessary due to increase in BER with each level. If PPM level and angular position are chosen such as to offer minimum compromise on the signal quality, the system has a potential to outperform other means of underwater communication. NLOS communication can be achieved for this mode of communication but its performance is not comparable to LOS communication. For deployment in a dynamic channel environment with changing transmitter and receiver positions, the alignment algorithm needs to be run on a regular basis to achieve reliable communication. Moreover, for scenarios with multiple optical paths between the transmitter and receiver, the alignment algorithm enables the receiver to point to the strongest direction of light arrival.

References

[1] H. M. Oubei et al., "Light based underwater wireless communications," Jpn. J. Appl. Phys., vol. 57, no. 8, July 18, 2018.

[2] D. Anguita, D. Brizzolara, G. Parodi, and Q. Hu, "Optical wireless underwater communication for AUV:Preliminary simulation and experimental results," in Proc. IEEE/OES Oceans, June 6-9, 2011, Santander. Spain: IEEE, 2011, pp. 1-5.

[3] M. Stojanovic, "Recent advances in high-speed underwater acoustic communications," IEEE Journal of Oceanic Engineering, vol. 21, no. 2, pp. 125-136, Apr. 1996.

[4] Y. Rong, S. Nordholm, and A. Duncan, "On the capacity of underwater optical wireless communication systems", Proc. Underwater commun. networking (UComms), Lerici, Italy, Sep. 2021.

[5] Z. Ghassemlooy, M. A. Khalighi, and D. Wu, "Channel modeling", in Visible light communications: Theory and applications, 1st ed., Z. Ghassemlooy, M. A. Khalighi, L. N. Alves, S. Zvanovec, Boca Raton, FL. USA: CRC-Press, Jun. 06, 2017, ch. 3, pp. 71–96.

[6] H. M. Oubei et al., "Underwater wireless optical communications: From system-level demonstrations to channel modelling," in 2017 22nd Microoptics Conference (MOC), Nov. 19-22, 2017, Tokyo. Japan: IEEE, 2017, pp. 34-35.

[7] S. Tang, Y. Dong, and X. Zhang, "Impulse response modeling for underwater wireless optical communication links," IEEE Trans. Commun., vol. 62, no. 1, pp. 226–234, Jan. 2014.

[8] Y. Kaymak, S. Fathi-Kazerooni, R. Rojas-Cessa, J. Feng, N. Ansari, M. Zhou, et al. "Beam with adaptive divergence angle in free-space optical communications for high-speed trains," arXiv preprint arXiv:1812.11233, Dec. 28, 2018.

[9] H. Zhang, Y. Dong, and X. Zhang, "On stochastic model for underwater wireless optical links," in Proc. 2014 IEEE/CIC Int. Conf. Commun. China (ICCC),no. 2, Oct. 13-15, 2014, Shanghai. China: IEEE, 2014, pp. 156–160.

[10] H. Zhang and Y. Dong, "General stochastic channel model and performance evaluation for underwater wireless optical links," IEEE Trans. Wirel. Commun., vol. 15, no. 2, pp. 1162–1173, Feb. 2016.

[11] H. Zhang, J. Cheng, and Z. Wang, "On integrated stochastic channel model for underwater optical wireless communications," in Proc. 2018 IEEE International Conference on Communications (ICC), May 20-24, 2018, Kansas City, MO. USA: IEEE, 2018, pp. 1-6.

[12] H. Zhang and Y. Dong, "Link misalignment for underwater wireless optical communications," in Proc. 2015 Advances in Wireless and Optical Communications (RTUWO), Nov. 5-6, 2015, Riga. Latvia: IEEE, 2015, pp. 215-218.

[13] F. Dong, L. Xu, D. Jiang, and T. Zhang, "Monte-carlo-based impulse response modeling for underwater wireless optical communication," Progr. Electromagn. Res., vol. 54, pp. 137–144, Feb. 2017.

[14] J. Sticklus, P. A. Hoeher and R. Rottgers, “Optical underwater communication: The potential of using converted green LEDs in coastal waters,” in IEEE Journal of Oceanic Engineering, vol. 44, no. 2, pp. 535-547, April 2019.
[15] Mazin Ali A. Ali, “Comparison of modulation techniques for underwater optical wireless communication employing APD receivers,” Research Journal of Applied Sciences, Engineering andTechnology, vol. 10, iss. 6, 2015, pp. 707-715.
[16] Carlson, A. Bruce, “Communication Systems: An Introduction to Signals and Noise in Electrical Communication”, Japan: McGraw-Hill, 1986.
[17] S. Trisno, “Design and analysis of advanced free space optical communication systems.” Order No. 3236735, University of Maryland, College Park, United States- Maryland, 2006.
[18] M. Sui and Z. Zhou, “The modified PPM modulation for underwater wireless optical communication,” 2009 International Conference on Communication Software and Networks, Chengdu, China, 2009, pp. 173-177.
[19] G. Sklivanitis, A. Gannon, S. N. Batalama and D. A. Pados, “Addressing next-generation wireless challenges with commercial software-defined radio platforms,” in IEEE Communications Magazine, vol. 54, no. 1, pp. 59-67, January 2016.
[20] P. Chen and Y. Rong, “A software-defined optical wireless OFDM system for underwater video communication”, Proc. MTS/IEEE OCEANS, Hampton Roads, Virginia, USA, Oct. 17-20, 2022.